

Surface-layer similarity in turbulent circular Couette flow

By MARTIN CLAUSSEN

Max-Planck-Institut für Meteorologie, Bundesstrasse 55, 2000 Hamburg 13, F.R.G.

(Received 29 July 1983 and in revised form 1 March 1984)

Smith & Townsend's (1982) experimental data on circular Couette flow are re-examined in the framework of surface-layer similarity theory. Surface-layer similarity of horizontally stratified shear flow is shown to have its counterpart in a narrow-gap Couette flow between concentric cylinders. Smith & Townsend's data of mean angular momentum and mean-velocity profiles in a region near a cylinder lend support to the applicability of Monin–Obukhov similarity to circular Couette flow. Only for flows of very high Reynolds numbers is a region of logarithmic variation of mean profiles found close to the cylinder wall. Because of curvature effects on the flow, the mean profiles deviate from the logarithmic profile as distance from the cylinder wall increases. For flows of sufficiently low Reynolds number, but still very high Taylor number, no logarithmic profile seems to exist; instead, profiles in the viscous region and in the outer region are connected to each other by a 'free-convection (rotation)' profile. From Smith & Townsend's data the velocity field is not observed to follow the prediction of 'free-convection' similarity; however, the 'free-convection' profile is found in the distribution of mean angular momentum.

1. Introduction

Smith & Townsend (1982) report measurements that have been made of a Couette flow between rotating cylinders. In their study, mean-velocity profiles and velocity spectra are reported over an extensive range of Taylor numbers which exceed the critical Taylor number by factors of 10^4 – 10^6 . This was for the inner cylinder rotating and the outer one fixed. Regarding the mean-velocity profiles at sufficiently high Taylor numbers, a large part of the wall layer was apparently unaffected by flow curvature, and a logarithmic distribution of mean velocity similar to that detected in channel flow was found. Smith & Townsend compare circular Couette flow and stratified flow with each other, and they argue that at distances from the wall smaller than a characteristic length, analogous to the Monin–Obukhov length of stratified flows, the flow is affected strongly by inertial forces, thus revealing logarithmic profiles. Although Smith & Townsend suggest application of Monin–Obukhov similarity to circular Couette flow, they do not formulate an analogous surface-layer similarity for Couette flow.

In atmospheric turbulence near the Earth's surface a considerable deviation from logarithmic profiles is observed at heights above ground much smaller than the Monin–Obukhov length (e.g. Monin & Yaglom 1971). We suppose that this trend may be seen from Smith & Townsend's data also, hence we have re-examined the data on mean velocity and mean angular momentum.

In §2 surface-layer similarity as originally proposed by Obukhov (1946) and by Monin & Obukhov (1954) is extended to circular Couette flow. Section 3 contains the application of the 'free-convection' scaling to circular Couette flow.

2. Surface-layer similarity

Surface-layer similarity of horizontally stratified fluids states that the mean temperature and wind fields depend only on the surface heat flux, a buoyancy parameter, the surface stress, and the height from the ground. By analogy, we suppose that the mean angular momentum and mean velocity fields in a circular Couette flow near a cylinder wall depend only on the flux G of angular momentum at the wall, a curvature parameter, the surface stress τ and the distance $r - R_1$ from the inner cylinder wall.

Comparison of the governing equation of steady-state Couette flow between concentric cylinders of radii R_1 (inner cylinder) and R_2 (outer cylinder) with those of steady Bénard convection between horizontal planes suggests that the term $2U/r^2$ is the analogue of the buoyancy parameter αg , where U is the mean velocity in the circumferential direction, α is the thermal expansion coefficient of the fluid and g is the acceleration due to gravity (see the Appendix). Furthermore, where molecular viscosity can be neglected, we have that

$$G = r^2 \overline{uw}, \quad (1)$$

\overline{uw} is the Reynolds stress.

From the above set of four variables we find a velocity scale

$$u_* = (\tau/\rho)^{\frac{1}{2}} \quad (2)$$

($\rho \equiv$ fluid density), an angular-momentum scale

$$M_* = |r^2 \overline{uw}|^{\frac{1}{2}} \quad (3)$$

and a lengthscale

$$L_* = -\frac{u_*^3}{2k(U/r^2)r \overline{uw}}. \quad (4)$$

The lengthscale L_* corresponds to the Monin–Obukhov length of stratified shear flow, where k is the von Kármán constant. We choose the sign of L_* such that a transport of angular momentum from the inner to the outer cylinder, indicating an unstable flow configuration, corresponds to a negative L_* , while a transport of angular momentum from the outer to the inner cylinder, indicating a stable flow configuration, is associated with a positive L_* . Analogous notation is used in boundary-layer meteorology. The curvature parameter $2U/r^2$ is assumed to be constant. In fact, $2U/r^2$ is far from constant; however, variation of this parameter in the surface layer is small compared with variation of $2U/r^2$ across the entire gap between cylinders. A typical or effective value is $2U_m/R_1^2$, where U_m is defined as the mean value of UR_1^2/r^2 within the surface layer. Using (1) and (4), we rewrite L_* as

$$|L_*| = \frac{G^{\frac{1}{2}}}{2kU_m}. \quad (5)$$

The length scale L_* in the form (5) was already proposed by Smith & Townsend as the analogue of the Monin–Obukhov length. From Smith & Townsend's data we estimate L_* to vary from $L_* \approx 1.3$ cm (for Reynolds number $Re \equiv U_1(R_2 - R_1)/\nu = 50000$; $U_1 \equiv$ peripheral velocity of inner cylinder, $\nu \equiv$ molecular viscosity) to $L_* \approx 1.2$ cm (for $Re = 8600$), i.e. from $L_*/(R_2 - R_1) \approx 0.17$ to $L_*/(R_2 - R_1) \approx 0.16$.

From the theory of dimensional analysis it follows that any variable being non-dimensionalized in terms of u_* , M_* , L_* and $r - R_1$ has to be a function of

$(r - R_1)/L_*$. For dimensionless gradients of angular momentum and velocity in the surface layer of circular Couette flow we have that

$$\frac{k(r - R_1)}{u_*} \frac{\partial(U_1 - U)}{\partial r} = \phi \left(\frac{r - R_1}{L_*} \right) \tag{6}$$

and that

$$\frac{k(r - R_1)}{M_*} \frac{\partial(U_1 R_1 - Ur)}{\partial r} = \phi_G \left(\frac{r - R_1}{L_*} \right) \tag{7}$$

ϕ and ϕ_G are universal functions depending only on the non-dimensional distance from the inner cylinder. Similar equations can be obtained for the surface layer near the outer cylinder.

In contrast with stratified shear flow, where we can regard temperature and velocity as independent quantities, the angular momentum Ur and the velocity U of circular Couette flow are not independent. Moreover, the scaling parameters M_* and u_* are not independent. M_* and u_* are related by

$$M_* = G^{\frac{1}{2}} = |r^2 \overline{uw}(r - R_1 = 0)|^{\frac{1}{2}} = |R_1^2 \tau / \rho|^{\frac{1}{2}} = u_* R_1. \tag{8}$$

Thus (6) and (7) can be used equivalently for scaling circular Couette flow data of mean velocity and angular momentum, and we can determine ϕ from ϕ_G , and *vice versa*.

For the mean velocity to be finite, the difference between (6) and (7)

$$U(r - R_1) = \frac{u_*}{k(r - R_1)} (r\phi - R_1 \phi_G) \tag{9}$$

(i.e. the difference $\phi - \phi_G$) has to become small as distance from the cylinder wall becomes small. In the limiting cases $r - R_1 \rightarrow 0$ and $R_1/R_2 \rightarrow 1$ the flow approaches a neutral flow configuration in which curvature effects become negligible in comparison with shear effects, and in which (6) and (7) become identical.

Figure 1 is a copy of Smith & Townsend's data (figure 2(d) in their paper). The straight line is given by

$$\frac{U_1 - U}{u_*} = \frac{1}{k} \ln \frac{r - R_1}{r_0 - R_1}, \tag{10}$$

where

$$r_0 - R_1 \equiv \frac{\nu}{u_*} e^{-A} \tag{11}$$

provides the link with Smith & Townsend's notation. The von Kármán constant k and the constant A are chosen so that $k = 0.4$ and $A = 2$. We have corrected Smith & Townsend's figure 2(d), since unfortunately their figure contained an erroneous factor of 2 in the von Kármán constant. Equation (10) can be found by integrating (6) and assuming $\phi = 1$; the case $\phi = 1$ corresponds to the neutral flow configuration. From figure 1 an increasing deviation from the logarithmic profile is seen for decreasing speed U of the inner cylinder and for increasing distance from the inner cylinder. We suppose shear effects on the flow to be dominant close to the cylinder wall, leading to a logarithmic profile; while rotational effects become more important as distance from the inner cylinder increases, causing a deviation from the logarithmic profile. Furthermore, for the three lowest Reynolds numbers no logarithmic profile seems to exist.

It should be emphasized that the case of a neutral flow configuration in circular Couette flow is a somewhat different one from stratified shear flow. A circular Couette

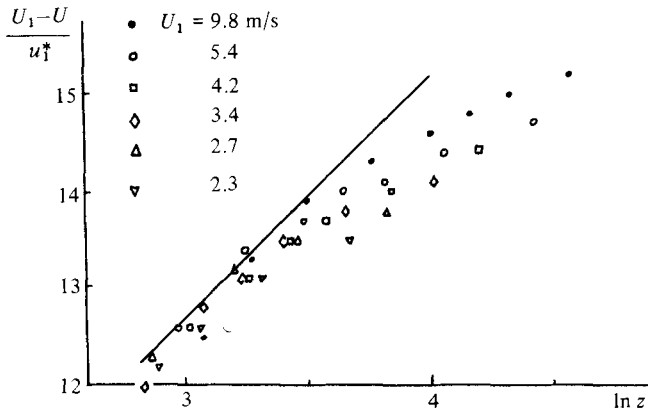


FIGURE 1. Non-dimensional plot of circumferential mean velocity versus distance from the inner-cylinder wall. The straight line has a slope of $1/k = 2.5$. Different symbols refer to different peripheral speeds of the inner cylinder. (Data for figure 1 are taken from figure 2(d) in Smith & Townsend (1982).)

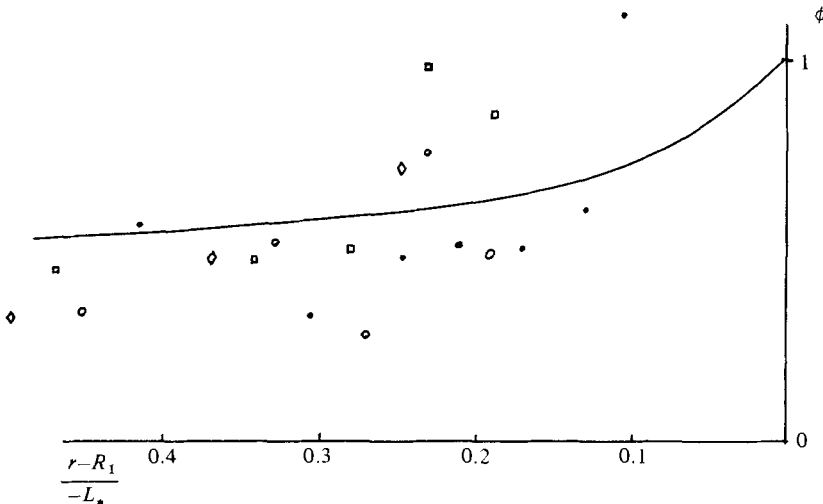


FIGURE 2. Non-dimensional plot of mean-velocity gradient versus distance from the inner-cylinder wall. The full line represents measurements in the atmospheric boundary layer by Dyer & Bradley (1982). For symbols see figure 1.

flow in which curvature effects are negligibly small corresponds to a plane Couette flow, i.e. to a circular Couette flow for which $R_1/R_2 \rightarrow 1$. Assuming a flow configuration in which the flux G of angular momentum at the cylinder wall vanishes (as the flux of temperature does in a neutrally stratified shear flow) implies a vanishing surface stress. No logarithmic profile is expected for such a flow configuration. On the other hand, in circular Couette flow in which $R_1/R_2 < 1$, a logarithmic profile is considered to be only an asymptotic profile in the limit of very high Reynolds number, and thus very high Taylor number $Ta \equiv [2(R_2 - R_1)/(R_2 + R_1)] Re^2$; curvature effects on the flow do not become completely unimportant.

Calculating the universal function ϕ , we take data from figure 1. Results are shown in figure 2. The full line represents recent observations of dimensionless gradients of mean velocity in the atmospheric boundary layer by Dyer & Bradley (1982). Our

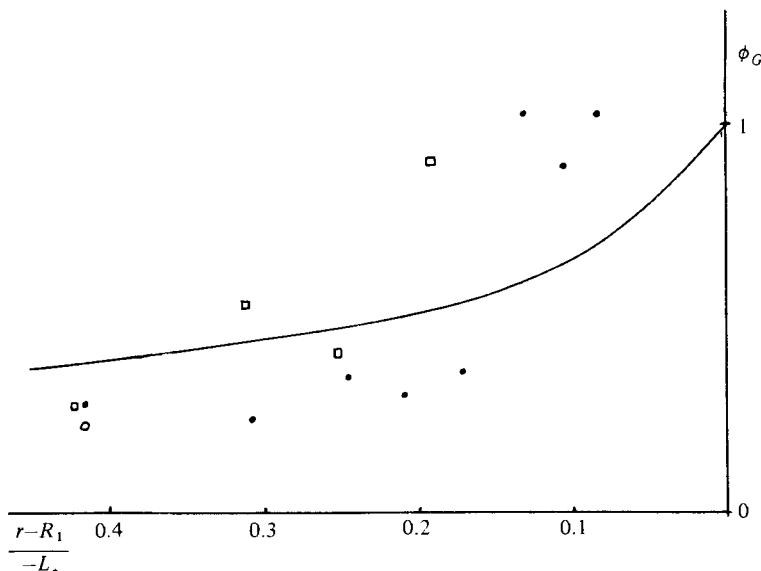


FIGURE 3. Non-dimensional plot of gradients of mean angular momentum versus distance from the inner-cylinder wall. The full line represents measurements of non-dimensional temperature gradients in the atmospheric boundary layer by Dyer & Bradley (1982). For symbols see figure 1.

calculations can be only a rough estimate on ϕ , since data are taken from Smith & Townsend's figure. However, our calculations indicate that circular-Couette-flow data follow the same trend as atmospheric data do: ϕ decreases as instability increases.

The non-dimensional gradient of angular momentum is calculated using data provided by Smith & Townsend (figure 1(b) in their paper). Again, data presented in figure 3 seem to follow the trend observed in atmospheric data of non-dimensional temperature gradients by Dyer & Bradley (1982). Our estimation also indicate ϕ_G to be smaller than ϕ , the difference $\phi - \phi_G$ increasing with increasing dimensionless distance from the cylinder wall.

3. 'Free-convection (rotation)' scaling

Another interesting analogy between circular Couette flow and stratified shear flow similarity arises assuming the surface stress to become unimportant in comparison with rotational (buoyant) effects on the flow. In this case the mean angular momentum and mean velocity fields are assumed to depend only on the flux of angular momentum at the cylinder surface, the curvature parameter, and the distance from the cylinder wall. From this set of three variables we find a velocity scale

$$u_t = \left(\frac{2U(r-R_1)}{r^2} \overline{r u w} \right)^{\frac{1}{3}} \tag{12}$$

and an angular-momentum scale

$$M_t = \left(\frac{r^2}{2U} \frac{1}{(r-R_1)} (\overline{r u w})^2 \right)^{\frac{1}{3}}. \tag{13}$$

We choose M_f rather than M_* as a scale in order to emphasize effects of curvature on the flow. Both scales are chosen to be similar to free-convection scales of stratified flow. The scales u_* , u_f and M_* , M_f are related to each other by

$$\frac{u_f}{u_*} = \left(\frac{r - R_1}{-kL_*} \right)^{\frac{1}{3}} \quad (14)$$

and

$$\frac{M_f}{M_*} = \left(\frac{r - R_1}{-kL_*} \right)^{-\frac{1}{3}}. \quad (15)$$

In contrast with free-convection scaling in stratified shear flow, we do find a lengthscale L_f given by

$$L_f = \frac{M_f}{u_f}. \quad (16)$$

However, like M_* and u_* , the scales M_f and u_f are not independent; thus gradients of angular momentum and velocity scaled with M_f , $r - R_1$ and u_f , $r - R_1$ respectively have to be constant. Therefore we can write

$$\frac{k(r - R_1)}{M_*} \frac{\partial(Ur)}{\partial r} = \frac{k(r - R_1)}{M_f} \frac{\partial(Ur)}{\partial r} \frac{M_f}{M_*} \sim \left(\frac{r - R_1}{L_*} \right)^{-\frac{1}{3}}, \quad (17)$$

$$\frac{k(r - R_1)}{u_*} \frac{\partial(U_1 - U)}{\partial r} = \frac{k(r - R_1)}{u_f} \frac{\partial(U_1 - U)}{\partial r} \frac{u_f}{u_*} \sim \left(\frac{r - R_1}{L_*} \right)^{\frac{1}{3}}. \quad (18)$$

Usually the state of free convection is associated with the limit of an infinitely large Monin–Obukhov length. But in the atmospheric boundary layer free-convection scaling seems to be applicable when heights above ground are of the order of the Monin–Obukhov length. We expect similar behaviour for circular Couette flow. In fact, Smith & Townsend's data indicate $(r - R_1)/kL_*$ to be of order unity or smaller throughout the surface layer.

Equations (17) and (18) seem to be inconsistent with each other, since we do not expect $Ur \sim (r - R_1)^{-\frac{1}{3}}$ and $U \sim (r - R_1)^{+\frac{1}{3}}$ simultaneously. However, since flow at high Taylor number but low Reynolds number is associated with convective flow, and since the angular-momentum field in circular Couette flow corresponds to the temperature field in convective flow, we suppose the 'free-convection' scaling to be applicable to the distribution of angular momentum rather than to that of velocity.

Figure 4 is a logarithmic plot of data copied in figure 1. The dashed straight line has a slope of $+\frac{1}{3}$. The full line represents the logarithmic profile. It can be seen that a significant region of logarithmic variation of velocity exists only for the flow of highest Reynolds number. A ' $(r - R_1)^{+\frac{1}{3}}$ region' as expected from similarity arguments is not found in figure 4. Neither the logarithmic profile nor the 'free-convection' profile seems to fit data for Reynolds numbers less than 50 000.

In figure 5 we have copied Smith & Townsend's data on mean angular momentum (figure 1(b) in their paper) using a logarithmic plot. The dashed straight line has a slope of $-\frac{1}{3}$. The full line represents the logarithmic profile. Obviously, only for the case of highest Reynolds number ($Re = 50\,000$) does a significant region of logarithmic variation of angular momentum exist. The region becomes considerably smaller as the Reynolds number decrease. No logarithmic variation is found for flows of Reynolds number less than $Re = 20\,000$. This is mentioned also by Smith & Townsend and is in agreement with earlier measurements by Taylor (1936). Instead, an extended ' $(r - R_1)^{-\frac{1}{3}}$ region' is observed which connects the outer layer in which $Ur \sim \text{const}$ and the region dominated by viscous processes for which $Ur \sim r - R_1$ is expected.

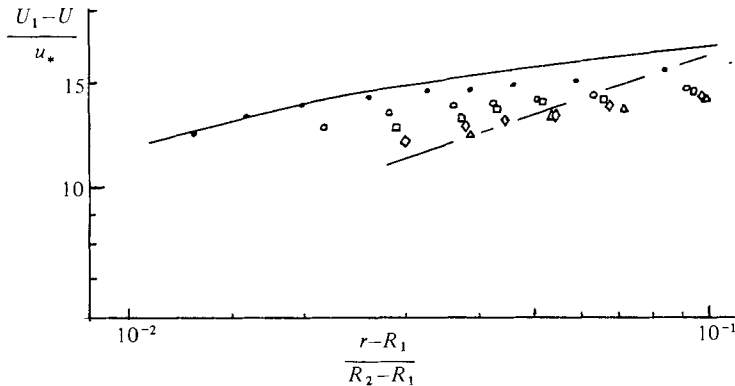


FIGURE 4. Non-dimensional logarithmic plot of mean velocity versus distance from the inner-cylinder wall. The dashed line has a slope of $+\frac{1}{3}$. The full line represents the logarithmic profile. For symbols see figure 1. (Data for figure 4 are taken from figure 1.)

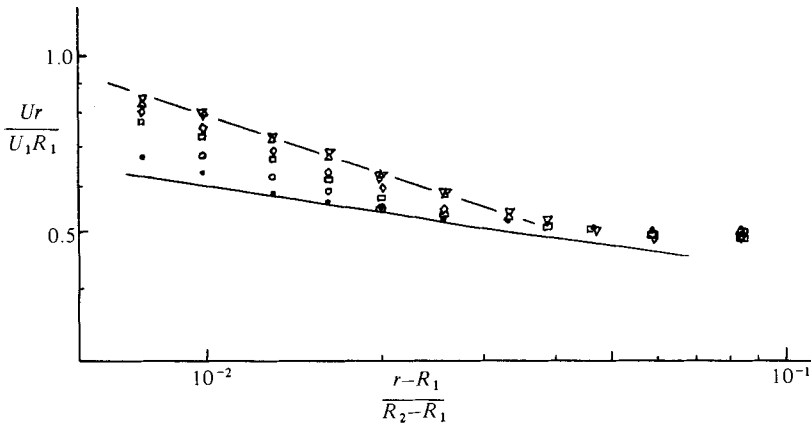


FIGURE 5. Non-dimensional logarithmic plot of mean angular momentum versus distance from the inner-cylinder wall. The dashed line has a slope of $-\frac{1}{3}$. The full line represents the logarithmic profile. For symbols see figure 1. (Data for figure 5 are taken from figure 1 (b) in Smith & Townsend (1982).)

4. Conclusion

Our study demonstrates how surface-layer similarity of horizontally stratified shear flow can be applied to Couette flow between concentric cylinders. Even the free-convection scaling is shown to have its counterpart in a narrow-gap Couette flow.

Re-examination of data provided by Smith & Townsend lends support to the applicability of Monin–Obukhov similarity to circular Couette flow: dimensionless gradients of mean velocity and mean angular momentum seem to be functions of a non-dimensional distance from a cylinder wall only. For flows of very high Reynolds number a region of logarithmic variation of mean velocity and mean angular momentum is found close to the cylinder wall. Because of curvature effects on the flow, mean-velocity and mean-angular-momentum fields deviate from the logarithmic profile as distance from the cylinder wall increases.

The present study sheds some light on the engineering practice of fitting surface-layer data on mean velocity and mean angular momentum by a logarithmic profile only. For instance, Wang & Gelhaar (1970) find two von Kármán constants: $k = 0.37$ for

the surface layer near the outer cylinder, and $k = 0.57$ near the inner cylinder. This is in contradiction with surface-layer similarity, which considers the von Kármán constant to be a universal constant. As mentioned above, the structure of the mean profile near a cylinder wall is more complicated. In an unstable flow configuration, mean profiles bend less than a logarithmic profile; therefore a 'logarithmic data fitting' yields a higher von Kármán constant. Furthermore, a purely logarithmic profile as in neutrally stratified shear flow cannot be expected in circular Couette flow.

Couette flow of sufficiently low Reynolds number ($Re < 20000$ in Smith & Townsend's experiment) but still high Taylor numbers corresponds to the case of vigorous, turbulent convection in stratified shear flow. For this case no logarithmic profile seems to exist; instead, profiles in the viscous region and in the outer region are connected to each other by a 'free-convection (rotation)' profile. From Smith & Townsend's data no such profile can be found for the mean-velocity field; however, the 'free-convection' profile is observed in the distribution of mean angular momentum. Interestingly enough, in the atmospheric boundary layer a velocity profile, as predicted from simple free-convection scaling, has not yet been measured, whereas the temperature distribution is reported to be close to the predicted profile (e.g. Businger 1973; Dyer & Bradley 1982). It could be argued that curvature influences the distribution of angular momentum stronger than that of velocity. From this, as the Reynolds number decreases, the onset of 'free-convection' is expected to be observed first in the distribution of angular momentum. Since Smith & Townsend's experiment provides a set of careful measurements, we suggest an extension of this experiment to lower Reynolds number in order to explore the scaling of 'free-convection'. In addition it should be interesting to examine whether or not the ' $(r-R_1)^{-\frac{1}{2}}$ region' close to the wall will be replaced by a ' $(r-R_1)^{-1}$ region', as predicted by Malkus (1979) for the limit of low Reynolds number but high Taylor number, and as observed by Townsend (1959) for laboratory convection.

Furthermore, our study raises the question as to why there is a rather abrupt change of profiles of mean angular momentum from $Ur \sim (r-R_1)^{-\frac{1}{2}}$ to $Ur \sim \text{const}$ (see figure 5). The next step in our investigation will be to ask whether Monin–Obukhov similarity will be applicable to a stable flow configuration, i.e. the inner cylinder stationary and the outer cylinder rotating. An additional, interesting investigation would be for a Couette flow with counter-rotating cylinders in which the gradient of angular momentum changes signs.

Finally, it should be understood that experiments on turbulent circular Couette flow are of particular value for understanding turbulence and transition to turbulence in stratified shear flow, since laboratory data or even atmospheric data of unstably stratified shear flow are difficult to obtain.

This work was undertaken while the author was at the Department of Meteorology and Physical Oceanography, MIT. He wishes to thank Professor W. V. R. Malkus for constructive comments and discussions.

Appendix

In steady-state Couette flow between concentric cylinders the equations for angular-momentum flux, for balance of mean-square angular-momentum fluctuations, and for balance of kinetic energy of the radial and axial velocity components are

$$r^2 \overline{uw} = G, \quad (\text{A } 1)$$

$$\overline{uw} \frac{d}{dr}(Ur) + \frac{1}{r} \frac{d}{dr}(\frac{1}{2} \overline{u^2 wr}) + \frac{\overline{u \partial p}}{r \partial \theta} = 0, \quad (\text{A } 2)$$

$$\frac{1}{r} \frac{d}{dr}(\overline{pwr} + \frac{1}{2} \overline{(v^2 + w^2) wr}) = \frac{2U}{r} \overline{uw} - \frac{\overline{u \partial p}}{r \partial \theta}. \quad (\text{A } 3)$$

We compare (A 1)–(A 3) with the equations for temperature flux, for balance of mean-square temperature fluctuations and for balance of turbulent kinetic energy in steady Bénard convection between parallel horizontal planes:

$$\overline{w\theta} = Q, \quad (\text{A } 4)$$

$$\overline{w\theta} \frac{dT}{dz} + \frac{d}{dz}(\frac{1}{2} \overline{w\theta^2}) = 0, \quad (\text{A } 5)$$

$$\frac{d}{dz}(\overline{pw} + \frac{1}{2} \overline{(u^2 + v^2 + w^2) w}) = \alpha g \overline{w\theta}, \quad (\text{A } 6)$$

where a is the coefficient of thermal expansion, T is the mean temperature at height z , θ is the temperature fluctuation, w is the velocity fluctuation in the vertical direction, and Q is the temperature flux transmitted per unit length of ground. Molecular viscosity and conductivity is neglected.

We choose G/r to be the analogue of Q , thus \overline{ruw} is the analogue of $\overline{w\theta}$. If $d(Ur)/dr$ is supposed to be the analogue of dT/dz , then we have to set $2U/r^2$ as the analogue of αg . This analogy is based on the assumption that the circumferential pressure gradient in circular Couette flow is negligibly small.

REFERENCES

- BUSINGER, J. A. 1973 A note on free convection. *Boundary-Layer Met.* **4**, 323.
- DYER, A. J. & BRADLEY, E. F. 1982 An alternative analysis of flux-gradient relationships at the 1976 ITCE. *Boundary-Layer Met.* **22**, 3.
- MALKUS, W. V. R. 1979 Turbulent velocity profiles from stability criteria. *J. Fluid Mech.* **90**, 401.
- MONIN, A. S. & OBUKHOV, A. M. 1954 Fundamentale Gesetzmäßigkeiten der turbulenten Vermischung in der bodennahen Schicht der Atmosphäre. *Akad. Nauk. SSSR, Geofis. Inst. Trudy* **151**, 163. [Transl. in *Sammelband zur statistischen Theorie der Turbulenz* (ed. H. Goering). Berlin, 1958.]
- MONIN, A. S. & YAGLOM, A. M. 1971 *Statistical Fluid Mechanics*, vol. 1. MIT Press.
- OBUKHOV, A. M. 1946 Turbulence in an atmosphere with a nonuniform temperature. *Trudy Inst. Teoret. Geofis. Akad. Nauk SSSR*. No. 1. [English Transl. in *Boundary-Layer Met.* **2** (1971), 7.]
- SMITH, G. P. & TOWNSEND, A. A. 1982 Turbulent Couette flow between concentric cylinders at large Taylor numbers. *J. Fluid Mech.* **123**, 187.
- TAYLOR, G. I. 1936 Fluid friction between rotating cylinders. I. Torque measurements. *Proc. R. Soc. Lond. A* **157**, 546.
- TOWNSEND, A. A. 1959 Temperature fluctuation over a heated horizontal surface. *J. Fluid Mech.* **5**, 209.
- WANG, A. K. M. & GELHAAR, I. W. 1970 Turbulent flow between concentric rotating cylinders. *Ralph M. Parsons Lab. for Water Resources and Hydrodynamics, MIT, Rep.* 132.